Alexandria Engineering Journal (2022) **61**, 9485–9494

HOSTED BY

ELSEVIER

Alexandria University

Alexandria Engineering Journal

www.elsevier.com/locate/aej
www.sciencedirect.com

Modelling of turbulent hydrogen-blended premixed flames using algebraic flame surface wrinkling closure for the Lewis numbers and mean local burning velocity

Siva PR Muppala

The Department of Mechanical Engineering, School of Engineering and Computing, Kingston University London, Roehampton Vale Campus, SW15 3DW. UK

Received 10 September 2021; revised 7 February 2022; accepted 10 March 2022

KEYWORDS

Turbulent premixed flames;
Lean mixtures;
Algebraic flame surface wrinkling;
Mean local burning velocity;
The Lewis numbers;
Bunsen flames

Abstract Hydrogen-blended fuel is of fundamental interest due to difficulties in modelling and its practical significance for the development of high-performance hydrogen combustion devices and safety technologies for the prediction and prevention of fire or explosion. In this analytical study, we validate an algebraic premixed turbulent model [13] for molecular transport effects in both spherical expanding methane flames enriched with hydrogen and Bunsen burner flames. Experiment comparisons are supported with theoretical ideas. Bunsen flames are measured at varied turbulence, equivalence ratios, temperatures, and pressures. We also consider other, very recent, experimental data [32] of similar fuel mixtures to support the trends.

In the study of outwardly evolving spherical expanding flames, we present three variants of this model, with two functions based on the Lewis number *Le*, and one based on the experimentally measured mean local flame burning velocity SFm. The Lewis number is significant in understanding the role of the diffusion of deficient reactants, which is particularly noticeable in blended fuels. The utilitarian part of this work is to demonstrate that the *Le*-based premixed turbulent models take into account the preferential diffusion effect, and to embed a term that quantifies turbulent flame speed explicitly for mixtures, for example, having the same unstretched burning velocity as the model input. We show that in the modelling of turbulent burning velocity, the use of SFm avoids the use of input parameters the unstretched laminar flame speed and the Lewis number. Moreover, we validate high-pressure experiments by Bagdanavicius [12] to show that the pressure has less significant impact on the Bunsen flames and, therefore, we model without the pressure term. The model correlates well with most of the data.

E-mail address: s.muppala@kingston.ac.uk

Peer review under responsibility of Faculty of Engineering, Alexandria University.

https://doi.org/10.1016/j.aej.2022.03.026

Nomenclature

a, b, c and d	are constants
A	averaged surface area
A_T	turbulent flame surface area
Ka	Karlovitz number
Le	the Lewis number, for both single and dual fuels
l_λ	Taylor's length scale
P	operating pressure
R_{et}	turbulent Reynolds number, based on lateral integral length scale
S_{L0}	unstretched laminar flame speed
SFm	mean local burning velocity of turbulent flame, a measured quantity
S_T	turbulent burning velocity
u'	turbulent intensity
u'/S_{L0}	turbulence intensity normalised by laminar burning velocity
S_T/S_{L0}	turbulent burning velocity normalised by laminar burning velocity
α	molecular thermal diffusivity
ϕ	equivalence ratio
δ_H	volume fraction of hydrogen
ρ_u	unburned density of the fresh mixture
ρ_b,	density of combustion products
v_0	molecular kinematic viscosity at 1 bar
v	molecular kinematic viscosity

1. Introduction

Due to political unrest around the world and increasing unprecedented environmental concerns due to alarming rates of global warming, the use of alternative sources of energy is of paramount importance today and in years to come. On this subject, we explore the suitability of an algebraic flame surface wrinkling model to measure the turbulent flame speed for hydrogen as an alternative fuel. Its unique flame characteristics are known to offer greater flame stability and the hydrocarbon flame characteristics can be attenuated by adding hydrogen even by leaner amounts. This non-carbon fuel reduces UHCs, NOx and CO to gain a higher percentage of hydrogen composition and enhances the reaction rate and thermal efficiency for leaner mixtures. Among these fuels, natural gas is a less polluting fuel, but its burning velocity is lower than with gasoline [1]. The impact on the characteristics of CH_4/air turbulent premixed flame by adding hydrogen is studied [2]. The primary reason for the rapid increase in turbulent burning velocity is more attributed to a reduction in the fuel Lewis number than that of a surge in laminar burning velocity with the addition of hydrogen. Power generation by means of H_2 addition not only diversifies the energy supply, but also minimises dependence on non-renewable fossil fuels. Hydrogen is unique, with its high-potential combustion characteristics and particularly wide range of flammability limits. Therefore, understanding the characteristics of hydrogen-doped and hydrogen turbulent flames is inevitable in development of safe premixed technologies for hydrogen [3].

The modelling of reaction rates is still seen to be a complex problem as turbulence and combustion are non-linearly interlinked. Moreover, a number of combustion models continue to evolve and many in the existing literature are less rigorously validated. The superimposition of hydrogen on hydrocarbon premixed flames poses a bigger modelling challenge. A number of studies, particularly in extensive 1-D flame simulations by [4], show that the behavioural characteristics of ultra-lean hydrogen mixtures is nontrivial (see Fig. 1). In this respect, experiments by Kido measure mean local burning velocity SFm, a substitute for the undisturbed laminar burning velocity for a plane flame S_{L0} [5]. This SFm is due to the local difference in the equivalence ratio induced by changes in the diffusional properties of the reactants, known as the preferential diffusion effect. In other words, SFm is a function of the mixture composition based on the different molecular diffusivities among the reactants, i.e. a function of fuel type, equivalence ratio, laminar burning velocity and turbulent intensity.

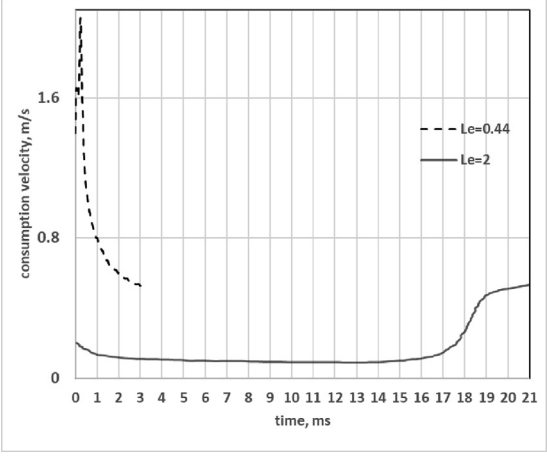

Fig. 1 Shows the variation of consumption velocity with time for the two Lewis numbers 0.44 and 2.0 (plots are redrawn, from Betev et al. [28]).

Based on earlier theoretical arguments, SFm is closely related to consumption velocity due to the local enrichment of the reaction zone at the leading edges [6].

One-dimensional simulations by Betev et al. [28] predict that $Le = 0.44$ mixtures with the highest consumption velocity 2.05 m/s are obtained with 0.236 ms, and a steady value $S_{L0}(\rho_u/\rho_b)$, reaching beyond 2 ms, whereas at $Le = 2.0$ at the flame expands slowly and increases suddenly after a long lapse. This figure will be referred later in the discussion. This highest consumption velocity is closer to the mean local burning velocity SFm, a quantity measured by Kido and his research group [7–9]. The leading point concept can be utilised to formulate a method in which flame propagation is controlled by flamelets

that advance further into the unburned mixture; thus, a state of highest consumption velocity is achievable, as shown in Fig. 1. This quantity is understood to be closely related to the measurable quantity mean local burning velocity.

In the same year (1998), Kido and Nakahara [10] proposed a similar concept that developed into a new model in which the preferential diffusion effects on S_T are quantifiable, by replacing S_{L0} with SFm in the premixed combustion model. However, measuring S_T, an important characteristic of premixed turbulent combustion, continues to be a challenge due to the complex interaction between turbulence and combustion. Shy et al. [11] state that the uncertainties in measuring values are predominantly due to very wide ranges of temporal and spatial scales in high-Reynolds-number chemically reacting flows.

Nakahara's work [9] investigates ways to measure S_T/S_{L0} as a function of (u'/S_{L0}) for various gaseous mixed fuels, mixture compositions, and enrichment of hydrogen, i.e. for *Le*, and Bagdanavicius [12] studies the influence of elevated inlet temperatures and pressures. For modelling analysis, we use the first author's premixed turbulent combustion model, the Algebraic Flame Surface Wrinkling (AFSW) model [13,14].

2. Experimental details

2.1. Experiments by Nakahara

We chose five different mixture compositions based on methane and propane with a hydrogen addition from experiments by Nakahara for the measurement of turbulent flame speed. The experimental set up, as shown in Fig. 2, consists of a spherical combustion chamber with a diameter of 100 mm for the turbulence level, approximately $u'/S_{L0} \sim 1.4$ and $u'/S_{L0} \sim 2.0$, corresponding to fan speeds of 1000 and 1400 rpm with an initial pressure of 0.101 MPa, and an initial temperature of 298 K. We present and discuss them in Sections 4.1 to 4.5.

They measure the mean local mean burning velocity SFm, a significant characteristic of premixed turbulent flames that quantifies the turbulent burning velocity without the need for the Le term and the unstretched laminar flame speed S_{L0} in the model. This quantity SFm takes into account the increase in the preferential diffusion with the increase in hydrogen addition [9]. Fig. 3 shows a neat quantitative relationship between SFm and S_T that are functions of the Le. To summarise, both quantities increase with the decrease in Le, and this increase is more dramatic for leaner mixtures of around $Le <= 0.4$, and SFm is a good replacement of S_{L0} to quantity S_T.

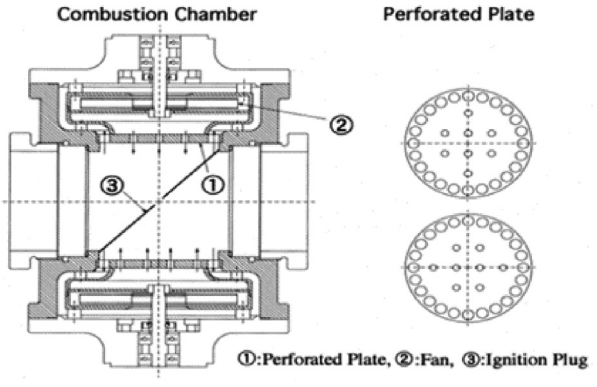

Fig. 2 The experimental set up of a combustion test rig [9].

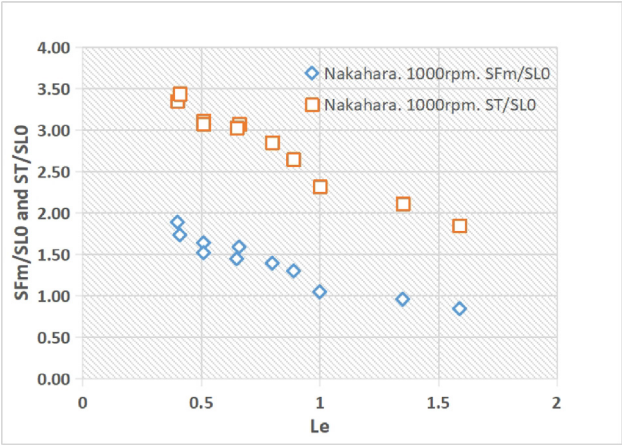

Fig. 3 This comparison shows the influence of Le on mean local burning velocity SFm and turbulent burning velocity S_T [9].

2.2. Experiments by Bagdanavicius (Leeds group)

Experiments by Bagdanavicius examine the variation of turbulent burning velocities, for different gaseous fuels at elevated temperatures and pressures, using a Bunsen burner. The flame is confined to a rectangular combustion chamber with a width and height of 150 mm in a high-pressure optical chamber (Fig. 4). Two sets of methane–hydrogen mixtures, 85% methane–15% hydrogen, and 70% methane–30% hydrogen is considered for the present analysis. Experiments were performed at three different temperatures (473 K, 573 K and 673 K) and two different pressures (3 bar and 7 bar). He inferred that hydrogen addition can enhance the turbulent burning velocity for lean mixtures. Further details can be found here [12].

3. Premixed turbulent combustion model

Considering the Borghi's flame regime diagram, most turbulent combustion models in the literature are derived for standard P and T conditions. The author of this paper has established an

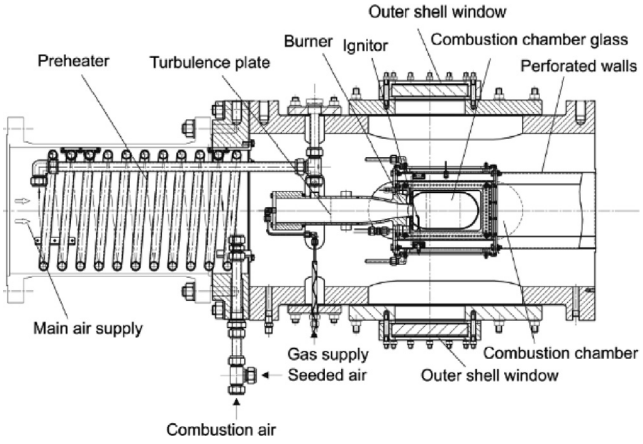

Fig. 4 Bunsen burner set up [12].

effective closure for premixed turbulent combustion called the AFSW model for pressures up to 3 MPa [13,15–17]. It could take an explicit fuel-type (or the Le) and pressure effects (see below Eqs. (1), (2), (3), (4)–(6)). This closure is modelled using the flame surface density of the reaction source term of the flame wrinkling ratio of A_T/A. The AFSW model shows S_T varies inversely with Le. This basic parameter $1/Le$ of the burning mixtures for $Le < 1$, is a manifestation of the increase in total flame surface area per unit volume, thus the turbulent flame speed and overall reaction rate. The model captures ultra-lean mixtures equally well, $Le < 0.5$ (Lipatnikov-2005). DNS by Trouve'– Poinsot [18] show the total reaction rate halves for methane/air mixtures $Le = 0.8$ to $Le = 1.2$.

Furthermore, the model Equ. 1 was modified to Equ. 2 using the exponential term, $e^{(Le\text{-}1)}$ based on the theoretical concept by Zel'dovich et al. [19] (also see [14,15] and see Table 3 in [20]). This new relation is relatively more congruent with several earlier experiments and numerical modelling studies [21,22]. This model is also independently validated in several studies [17,23,24]. This formulation is given in various closures.

$$\frac{S_T}{S_{L0}} = 1 + \left(\frac{\sqrt{2}}{3}\right)\left(\frac{1}{Le}\right) Re_t^{0.25}\left(\frac{u'}{S_{L0}}\right)^{0.3}\left(\frac{v_0}{v}\right)^{0.2} \tag{1}$$

$$\frac{S_T}{S_{L0}} = 1 + \left(\frac{\sqrt{2}}{3}\right)\left(\frac{1}{e^{(Le-1)}}\right) Re_t^{0.25}\left(\frac{u'}{S_{L0}}\right)^{0.3}\left(\frac{v_0}{v}\right)^{0.2} \tag{2}$$

$$S_T = SFm + \frac{\sqrt{2}}{3}\left(Re_t^{0.25}\right)(u')^{0.3}(SFm)^{0.7} \tag{3}$$

Here, SFm is related to the Karlovitz number, Ka = (u'/l_λ) (α/SFm^2), where l_λ is Taylor's length scale, α is molecular thermal diffusivity. Here, v_0/v is the inverse of the molecular kinematic viscosity normalised by the same quantity at operating pressure with v_0 at 1 atm, which accommodates additional pressure influence. According to the flame regime diagram, unity Karlovitz number represents the boundary between the thin reaction zone and the corrugated regime.

The model in Eq. (3) show an increase in fluctuating velocity u' and characteristics length scale (integral length scale) l_x increases S_T. Eqs. (1), (2), (3) shows that the S_T is proportional to u'$^{0.55}$, which is closer to Damköhler's expression$S_T \propto u'^{0.5}$.

This algebraic expression Eq. (1) or Eq. (2) in generic form, Equ. 4.

$$S_T = S_{L0} + (pre - constant)\, u'^a\, l_t^b\, S_{L0}^c\, v^d \tag{4}$$

gives combinations among exponents a + c + d = 1; and a + b + c + 2d = 1, using a = 0.55; b = 0.25; c = 0.7; and d = –0.25. This implies that the equation is homogeneous and dimensionally consistent among the exponential constants; a combination of these constants give a sum equal to unity, the pre-constant taking the effect of fuel, $\frac{0.46}{Le}$.

Using the Karlovitz number in terms of S_{L0}.

$$Ka = 0.157 Re_t^2\left(\frac{u'}{S_{L0}}\right)^2$$

Equ.(1)/(2) can be transformed to.

$$S_T = S_{L0} + 18.65 Ka^2\left(\frac{u'}{S_{L0}}\right)^{-1.7}\left(\frac{v_0}{v}\right)^{0.2} \tag{5}$$

This expression, Eq. (5) $S_T = f(Ka)$ is similar to that resulting from the Kido database. A fit model devised from this database is split to identify two flame characteristics, the straight-line and a flat curve (1– Ka^2), which yield the condition of the flame quenching at Ka = 1.0.

$$S_T = \left(S_L + \frac{\sqrt{2}}{2}\alpha u'\right)(1 - Ka_L{}^2) 0 < Ka_L \le 0.5 \tag{6}$$

An effort is made to show that Eq. (5) can be re-constructed to form an analogy with Eq. (6), an empirical fit of the experimental data given by Nakahara [7]. However, the present numerical model could not demonstrate the quenching condition. In other words, more study is required to include stretch effects in the model to show the level of steadiness that the turbulent flame speed has to achieve, which should not increase beyond a certain turbulence level or state of flame-quenching.

The quantification of the likelihood of flame quenching could not be inferred from this reconstructed numerical model, Eq. (5). This may require the inclusion of complex stretch effects into the current model. However, the model works equally well compared to Eq. (6) for the present measured data, as discussed below using the various closures, Eqs. (1) to (3).

However, the significance of the Lewis number in leaner mixtures on premixed turbulent flames is extraordinarily reviewed by Lipatnikov and Chomiak [25]. They assert that Le is more effective than the Markstein number Ma for turbulent combustion modelling as well as perturbation, which is applicable to turbulent flames. The AFSW model uses an effective Lewis number Le_{eff} instead of Ma.

In practice, when modelling with the Markstein number, Ma has proven difficult to obtain without significant experimental or numerical studies. Moreover, Ma is in several forms due to a wide variation in their values among independent studies [26]. Therefore, the turbulent burning velocity correlations S_T mostly based on the Le that can be obtained directly from mixture properties. One of the ways to estimate effective Lewis number Le_{eff}, for example by using the Dinkelacker model $\frac{1}{Le_{eff}} = \frac{D^*}{\alpha} = \frac{x_1 D_1}{\alpha} + \frac{x_2 D_2}{\alpha} = \frac{x_1}{Le_1} + \frac{x_2}{Le_2}$ [15]. Here, α is molecular heat diffusivity and D is molecular mass diffusivity. However, in this study, we use the values provided from the experiments.

In the AFSW model, S_T is dominated by three parameters, normalised turbulent velocity u'/S_{L0}, the turbulent Reynolds number Re and the Le. However, a very recent experimental study by Lhuillier et al. [27] partly modifies the AFSW model with a multiplication factor, modulus of Markstein number to the power 0.06, shows that the model correlates very well with their expanding ammonia flames enriched with H_2, and concludes that S_T/S_{L0} increases with the decrease of Le_{eff} due to the onset of preferential diffusion, which *amplifies the accelerating effects of turbulence-induced flame wrinkling*.

In the following, we examine S_T using the AFSW model to show that the model captures the experimental findings for each data point for the addition of hydrogen to methane/air mixtures under lean conditions, for the Le range 0.4 to 1.59, shown in Table 1. The model works equally brilliantly by replacing Le and S_{L0} with SFm, a flame quantity that quantifies the preferential diffusion effect, due to *different molecular diffusivities among reactants*. We extend the discussion to independent set of data from Bunsen flames.

Table 1 Properties of fuel mixtures and of test conditions of spherical expanding flames at $\phi = 0.5$. Experiments by Nakahara (personal communication).

ϕ	δ_H	C_3H_8	CH_4	H_2	O_2	N_2	S_{L0} (cm.0/s)	α_0 (mm^2/s)	ν (mm^2/s)	Le	Re_t (1000 rpm)	u'/S_{L0}	Re_t (1400 rpm)	u'/S_{L0}
0.5	0	–	1	0.0	4.0	9.2	25.0	21.1	15.6	0.89	63.0	1.404	88.20	1.97
0.5	0.2	–	0.8	0.2	3.4	8.4	24.8	22.2	15.8	0.80	62.2	1.415	87.08	1.98
0.5	0.5	–	0.5	0.5	2.5	7.5	25.0	24.3	16.2	0.66	60.6	1.405	84.84	1.97
0.5	0.8	–	0.2	0.8	1.6	7.2	25.2	26.9	16.7	0.51	58.9	1.395	82.46	1.95
0.5	1.0	–	0	1.0	1.0	6.9	25.1	29.2	17.2	0.40	57.4	1.402	80.36	1.96
0.4	0.8	–	0.2	0.8	2.0	6.9	25.2	26.9	16.7	0.51	58.9	1.395	82.46	1.95
0.5	0	1.0	–	0.0	10	25	25.0	19.6		1.59	66.4	1.402	92.96	1.96
0.5	0.2	0.8	–	0.2	8.2	20	25.2	20.1	14.9	1.35	65.9	1.391	92.26	1.95
0.5	0.5	0.5	=	0.5	5.5	14	25.4	21.4	15.2	1.00	64.6	1.381	90.44	1.93
0.5	0.8	0.2	–	0.8	2.8	8.8	25.3	24.6	15.9	0.65	61.6	1.388	86.24	1.94
0.5	1.0	0.0	–	1.0	1.0	6.6	24.9	29.5	17.2	0.41	57.1	1.413	79.94	1.98

4. Results and Discussion

4.1. = 0.5: CH_4 /H_2 for $u'/S_{L0} \sim 1.4$ and $u'/S_{L0} \sim 2.0$, with 1/Le & $\frac{1}{e^{(Le-1)}}$ term

We analytically investigate spherical expanding flames using AFSW model (Eq. (1), (2), (3) & Eq. (2)), for the influence of hydrogen on methane and propane mixtures at turbulence fan speeds 1000 rpm (u'=0.35) and 1400 rpm (u'=0.49), for varied Lewis numbers, given in Table 1. The propane mixtures will be presented from Section 4.3.

Fig. 5a and b, in the vicinity of $u'/S_{L0} \sim 1.4$, show variation in S_T/S_{L0} due to the influence of the preferential diffusion, more predominantly for Le < 1 mixtures, corroborates with the hypothesis by Zel'dovich [19] as cited in Betev et al. [28]. The model values from Eq. (2). with the term $1/e^{(Le-1)}$ is based on this idea and, therefore, it complements these experiments very well. It shows that, for Le < 1, from a physics point of view, the radius of the minimum critical radius with respect to laminar flame thickness decreases, which helps propagate the flame faster, and tends to become more radical the leaner the mixtures become under the influence of preferential diffusion. Similarly, Peters and Williams' (1981) concept states that the local burning rate in the flamelets and their local extinction depend substantially on *Le*. Poinsot and Trouvé [18] show that *Le* < 1 flames are thermo-diffusively unstable causing higher heat release and the generation of a higher flame area (also see recent studies [29,30]).

Note that the data points (i) and (ii) overlap for both the experiment and the model.

Fig. 5a shows the results for Eq. (1), (2), (3), with an over prediction for one data point (iii), whereas Eq. (2) captures this experimental trend near perfectly for all the *Le* values ranging between 0.4 and 0.89.

Fig. 6a and b show slightly higher turbulence $u'/S_{L0} \sim 2$, and the model with $1/Le$ term continues to show a similar pattern to that in Fig. 5a and b. However, Eq. (2) with $1/e^{(Le-1)}$, yields a very good qualitative trend for all values, but partly under predicts within an acceptable level.

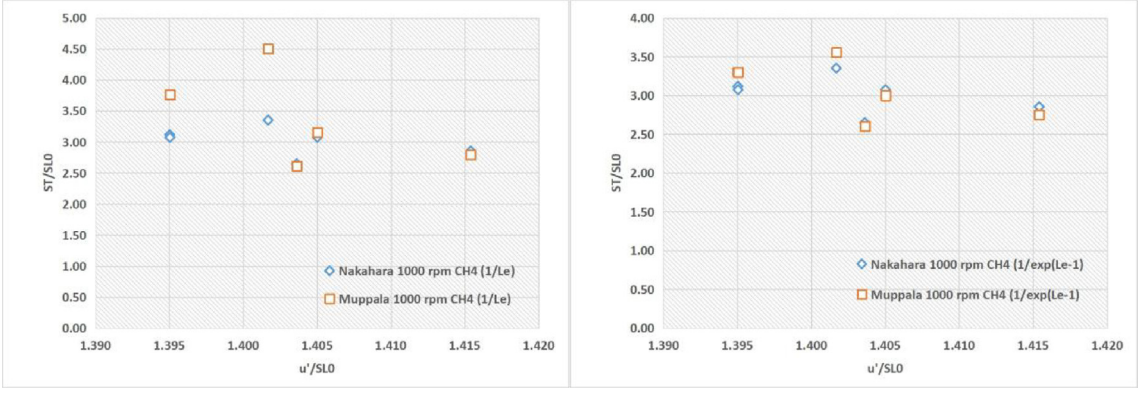

Fig. 5 a. (L) (Eq. (1)) and 5b (R) (Eq. (2)). For 1000 rpm shows a comparison between the Nakahara experiment and the Muppala model for S_T/S_{L0} vs. u'/S_{L0} for CH_4/H_2 mixtures at ϕ=0.5, except for one piece of data at ϕ – 0.4. From Table 1 (L to R): (i) ϕ – 0.4 - (S_{L0} = 25.2, *Le* = 0.5, Re = 58.9) - δ_H _ 0.8; (ii) ϕ – 0.5 – (S_{L0} = 25.2, *Le* = 0.5, Re = 58.9) - δ_H _ 0.8; (iii) (S_{L0} = 25.1, *Le* = 0.4, Re = 57.4) - δ_H _ 1; (iv) (S_{L0} = 25, *Le* = 0.9, Re = 63) - δ_H _ 0; (v) (S_{L0} = 25, *Le* = 0.7, Re = 60.6) - δ_H _ 0.5; (vi) (S_{L0} = 24.8, *Le* = 0.8, Re = 62.2) - δ_H – 0.2.

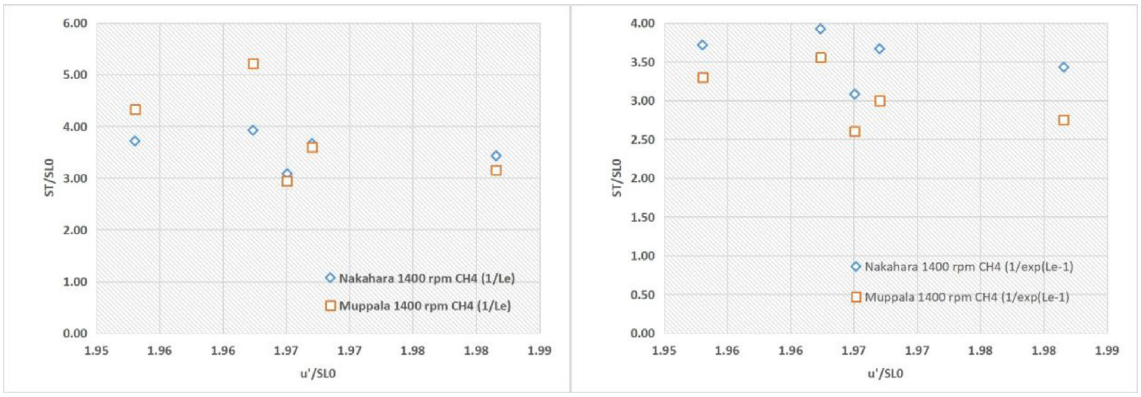

Fig. 6 a (L) (Eq. (1)) and 6b(R) (Eq. (2)). (i) (S_{L0} = 25.2, *Le* = 0.5, Re = 58.9) - $\delta_{\mathbf{H}}$ _ 0.8; (ii) (S_{L0} = 25.1, *Le* = 0.4, Re = 57.4) - $\delta_{\mathbf{H}}$ _ 1; (iii) (S_{L0} = 25, *Le* = 0.9, Re = 63) - $\delta_{\mathbf{H}}$ _ 0; (iv) (S_{L0} = 25, *Le* = 0.7, Re = 60.6) - $\delta_{\mathbf{H}}$ _ 0.5; (v) (S_{L0} = 24.8, *Le* = 0.8, Re = 62.2) - $\delta_{\mathbf{H}}$ _ 0.

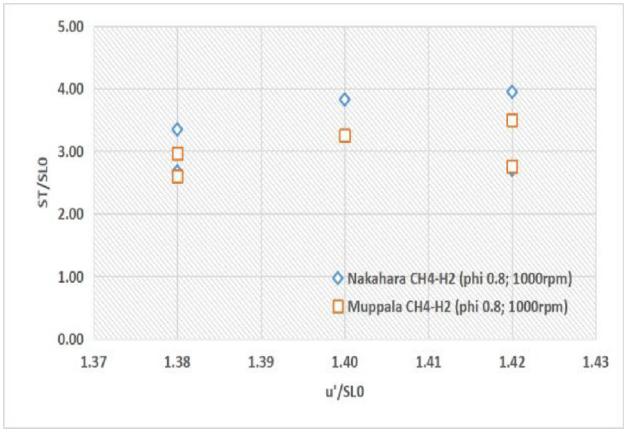

Fig. 7 (Eq. (2)) shows the variation of S_T/S_{L0} with *Le* (conditions given in Table 2). The data points from L to R: i) (S_{L0} = 25.4, *Le* = 0.67, *Re* = 60.4); ii) (S_{L0} = 25.3, *Le* = 0.89, Re = 63.1); iii) (S_{L0} = 25.1, *Le* = 0.53, *Re* = 58.2); iv) (S_{L0} = 24.7, *Le* = 0.42, Re = 56.5); v) (S_{L0} = 24.8, *Le* = 0.80, *Re* = 62.2).

4.2. ϕ = 0.8, CH_4/H_2 at $u'/S_{L0} \sim 1.4$, with $\frac{1}{e^{(Le-1)}}$ term

For ϕ = 0.8, all lean CH_4/H_2 mixtures are prepared in the vicinity of $u'/S_{L0} \sim 1.4$ (Fig. 7). The predominant factor that affects S_T/S_{L0} is due to the preferential diffusion in lean mixtures (Le < 1), despite lowering the Reynolds number, as shown in Table 2. The model gives an excellent agreement with the measurements. At u'/S_{L0} = 1.42 for Le = 0.42 gives the maximum S_T/S_{L0} for the given data. This can be explained through the higher enrichment of hydrogen leading to higher diffusivity of deficient reactant into the convex part of unburned mixtures, which indicates that a leaner mixture yields a higher burning velocity. Karpov and Severin [6] state that a smaller *Le* in the range *Le* < 1, the mixtures burn at higher rates and the cellular structure becomes more pronounced.

Fig. 7 shows a consistent variation with Le, with higher S_T/S_{L0} for the lower *Le*. The model values for C_3H_8/H_2 mixtures (not shown here), for *Le* = 0.42 to 0.89, indicate that a similar inverse relationship can be seen between S_T/S_{L0} and *Le*.

4.3. ϕ = 0.5: C_3H_8 /H_2 mixtures, for $u'/S_{L0} \sim 1.4$ and $u'/S_{L0} \sim 2.0$, with 1/Le & $\frac{1}{e^{(Le-1)}}$ term

For higher hydrocarbon, propane five fuel mixture compositions with the addition of hydrogen varying from 0%, 20%, 50%, 80% and 100% hydrogen mixtures are prepared (see Table 1). Fig. 8a and b show that the AFSW model predicts extremely well for all data points, except for one that it over predicts. For *Le* = 0.4 and predictably even leaner mixtures, the hydrogen flame shows special characteristics in that the constant limit of consumption velocity increases more than for *Le* > 0.4 (as shown in Fig. 1). This transport phenomenon of expanding hydrogen flames is extensively discussed by Lipatnikov and Chomiak [4].

A comparison between Fig. 5a (L) and Fig. 8a (L) provides evidence that the burning rate of methane mixtures is relatively much higher than propane mixtures with corresponding values. The results shown are the variations for $S_T \propto \frac{1}{e^{(Le-1)}}$.

Nakahara et al. [9] explain that for lean hydrogen-added mixtures, the diffusion of lighter fuel is more predominant towards the convex flame of the unburned mixture due to preferential diffusion. From their numerical simulations, Brower et al. [31] show that S_T increases two-fold when 50% of H_2 is added to CH_4/air mixtures.

Fig. 9a(L) and b(R) show for a higher level of turbulence $u'/S_{L0} \sim 2.0$ the model yields exact predictions for some data and shows a sudden jump for *Le* = 0.4 for the reasons mentioned above. Fig. 9b shows a very similar trend to Fig. 6b.

In the following, for the fuel/air mixtures of various equivalence ratios and Bunsen flames, we use the model that is more characteristic of the outwardly expanding spherical flames. See Eq. (2).

4.4. Validation of ϕ = 0.5, 0.6 & 0.8 C_3H_8/H_2 mixtures at different turbulence levels, using model $S_T \propto \frac{1}{e^{(Le-1)}}$

Here, we compare the model with the experiment using higher order hydrocarbon, propane/air mixtures enriched with hydrogen for the two varying turbulence levels given in Table 2.

Table 2 Properties of CH_4/H_2/air mixtures, for $\phi = 0.8$ and 1000 rpm, where δ_H is a hydrogen fraction.

δ_H	Components				u' (cm/s)	S_{L0} (cm/s)	Le	1000 rpm	
	CH_4	H_2	O_2	N_2				u'/S_{L0}	Re_l
0.0	1.0	0.00	2.50	9.63	34.91	25.3	0.89	1.38	63.1
0.2	0.8	0.20	2.13	8.93	35.22	24.8	0.80	1.42	62.2
0.5	0.5	0.50	1.56	7.42	35.05	25.4	0.67	1.38	60.4
0.8	0.2	0.80	1.00	6.45	35.14	25.1	0.53	1.40	58.2
1.0	0.0	1.00	0.63	6.13	35.07	24.7	0.42	1.42	56.5

Table 3 Properties of Mixtures and Test conditions for the three compositions $\phi = 0.5$, 0.6, 0.8 of propane/air mixtures (plotted in Figs. 10 to 12) (Nakahara et al. personal communication).

	Components (mol)				S_{L0} (cm/s)	α (mm^2/s)	ν (mm^2/s)	Le	Fan speed 1000 rpm		Fan speed 1400 rpm	
ϕ	H_2	C_3H_8	O_2	N_2					u'/S_{L0}	Re_t	u'/S_{L0}	Re_t
0.5	0.8	0.2	2.80	10.53	15.60	24.1	15.9	0.64	2.24	61.8	3.14	92.4
0.5	1.0	0.0	1.00	3.76	69.60	34.2	18.3	0.47	0.51	53.9	0.71	80.5
0.6	0.8	0.2	2.33	8.80	24.10	24.7	15.9	0.66	1.46	61.5	2.04	91.9
0.6	1.0	0.0	0.83	8.78	104.40	36.6	18.8	0.50	0.23	52.4	0.33	78.2
0.8	0.0	1.0	6.25	3.14	30.00	19.4	14.6	1.57	1.17	66.9	1.64	100.0
0.8	0.8	0.8	5.13	19.28	30.70	20.0	14.8	1.34	1.14	66.4	1.60	99.2
0.8	0.5	0.5	3.44	12.93	35.10	21.5	15.1	1.00	1.00	64.9	1.40	97.0
0.8	0.2	0.2	1.75	6.58	53.90	25.9	16.1	0.68	0.65	60.9	0.91	91.0

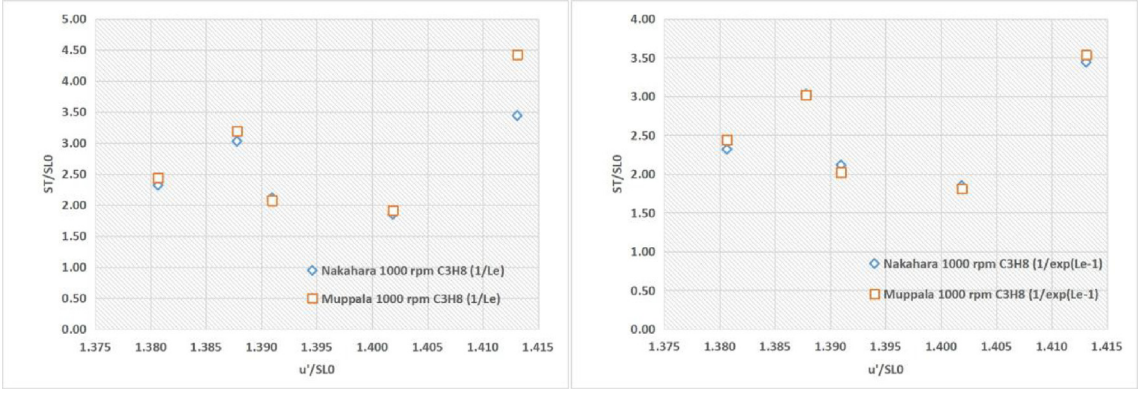

Fig. 8 a (L) (Eq. (1)) and Fig. 8b(R) (Eq. (2)). (i) $\delta_H = 0.5$ ($S_{L0} = 25.4$, $Le = 1$, Re = 64.6) (ii) $\delta_H = 0.8$ ($S_{L0} = 25.3$, $Le = 0.7$, Re = 61.6) (iii) $\delta_H = 0.2$ ($S_{L0} = 25.2$, $Le = 1.4$, Re = 65.9) (iv) $\delta_H = 0$ ($S_{L0} = 25$, $Le = 1.6$, Re = 66.4) (v) $\delta_H = 1$ ($S_{L0} = 24.9$, $Le = 0.4$, Re = 57.1).

Fig. 10 shows the model and Eq. (2) predicts the experimental trend that can be seen in two partitions, a flatter behaviour beyond $u'/S_{L0} >= 1$, and an increase in turbulent burning velocity. The figure also shows S_T/S_{L0} increases with a decrease in the Lewis number, and it is even more significant with the corresponding increase in turbulence. This is a fascinating phenomenon in premixed turbulent flames, which is generally seen as a difficult part of modelling. Nevertheless, as shown in Fig. 11, the AFSW model captures the qualitative and quantitative trends very well and for higher turbulence and *Le* ranging from 0.47 to 1.57.

4.5. $\phi = 0.5$. Evaluation of S_T/S_{L0} by replacing 'S_{L0} and Le terms' with SFm

Fig. 3 shows a cosmic connection between SFm and S_T. By modifying the combustion model by replacing terms containing 'S_{L0} and *Le*' with a measured quantity SFm, which takes into account the preferential diffusion, an excellent agreement is given for the whole range of experimental data, as shown in Fig. 12. The significance of this quantity is discussed for Fig. 1, and in the Kido database.

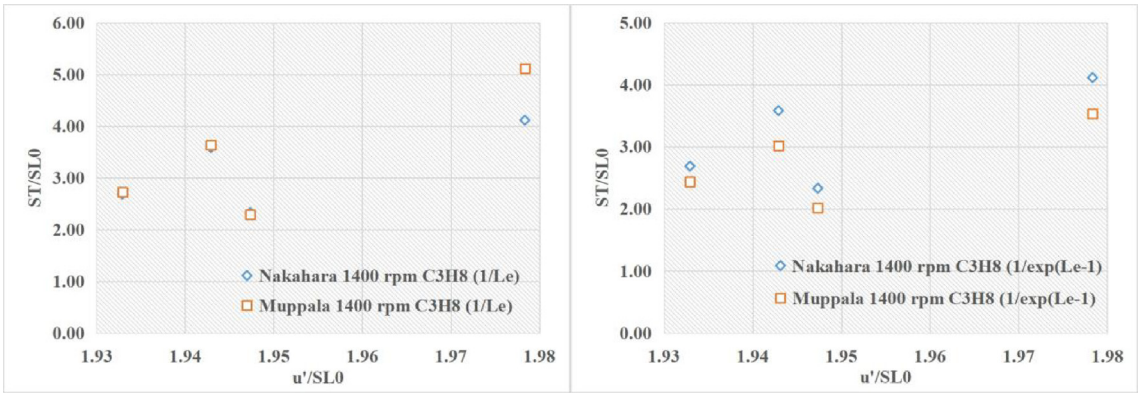

Fig. 9 a(L) (Eq. (1)) and 9b(R). (Eq. (2)) (i) (S_{L0} = 25.4, *Le* = 1, Re = 64.6) - δ_H _ 0.5; (ii) ϕ (S_{L0} = 25.3, *Le* = 0.7, Re = 61.6) - δ_H _ 0.8; (iii) (S_{L0} = 25.2, *Le* = 1.4, Re = 65.9) - δ_H _ 0.2; (iv) (S_{L0} = 24.9, *Le* = 0.4, Re = 57.1) - δ_H _ 1.

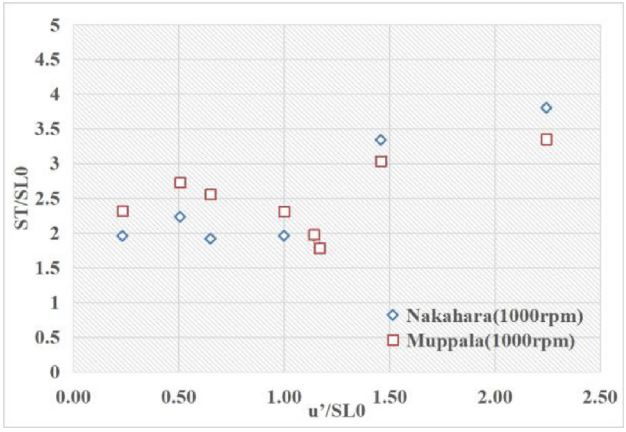

Fig. 10 (Eq. (2)). Comparison between experiment and AFSW model, for S_T/S_{L0} vs. u'/S_{L0} for C_3H_8/H_2 mixtures at ϕ = 0.5, 0.6, 0.8 for 1000 rpm ($S_T \propto \frac{1}{e^{(Le-1)}}$). i).($S_{L0}$ = 104.4, Le = 0.50, Re = 52.4); ii) (S_{L0} = 69.6, Le = 0.47, Re = 53.9); iii) (S_{L0} = 53.9, Le = 0.68, Re = 60.9); iv) (S_{L0} = 35.1, Le = 1, Re = 64.9); v) (S_{L0} = 30.7, Le = 1.34, Re = 66.4) vi) (S_{L0} = 30, Le = 1.57, Re = 66.9); vii) (S_{L0} = 24.1, Le = 0.66, Re = 61.5); viii) (S_{L0} = 15.6, Le = 0.64, Re = 61.8) (See Table 3).

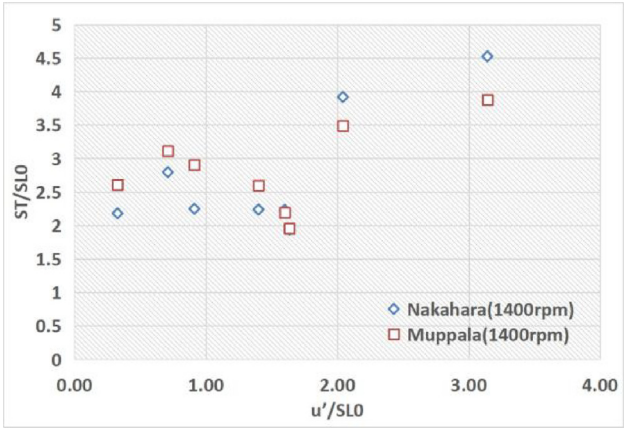

Fig. 11 (Eq. (2)). Comparison between experiment and AFSW model, for S_T/S_{L0} vs. u'/S_{L0} for C_3H_8/H_2 mixtures at ϕ = 0.5, 0.6, 0.8 for 1400 rpm ($S_T \propto \frac{1}{e^{(Le-1)}}$). i) ($S_{L0}$ = 104.4, Le = 0.50, Re = 78.2); ii) (S_{L0} = 69.6, Le = 0.47, Re = 80.5); iii) (S_{L0} = 53.9, Le = 0.68, Re = 91); iv) (S_{L0} = 35.1, Le = 1, Re = 97); v) (S_{L0} = 30.7, Le = 1.34, Re = 99.2) vi)(S_{L0} = 30, Le = 1.57, Re = 100); vii) (S_{L0} = 24.1, Le = 0.66, Re = 91.9); viii) (S_{L0} = 15.6, Le = 0.64, Re = 92.4).

5. Bagdanavicius data: CH_4 – H_2 mixtures at various equivalence ratio and turbulence

We analyse and validate a different set of data for turbulent burning velocities measured by Bagdanavicius [12] on a ∅ 25-mm Bunsen burner for pure methane and two mixed 85% CH_4–15% H_2, and 70% CH_4–30% H_2 mixtures at elevated temperatures 473 K and 673 K and pressures 3 bar and 7 bar. This experiment shows no evidence of an increase in S_T/S_{L0} at elevated pressures. Therefore, the pressure term in Eq. (1), (2), (3) is dropped. For further validation, we include recent data at standard pressure and temperature conditions from [32], which show that both have good qualitative trends. For two data points, 1.5 < u'/S_{L0} < 2.0, a considerable deviation is seen, as shown in Fig. 13. This is possibly attributed to high integral length scale and the model seems to over predict. Otherwise, the rest of the data are largely congruent with the experiment. The model predicts well even for high turbulence, $u'/S_{L0} \sim 3.0$.

Fig. 14 also gives a consistent summarisable correlation with independent experiments by Zhang et al. [32], which were carried out for natural gas mixed with 10% H_2 and 30% H_2 mixtures. These data fall on either side of Bagdanavicius' data. A smooth U-curve is possible (not shown) among both experiments and model values, with the lowest around $u'/S_{L0} \sim 1.3$.

They argue that with the addition of hydrogen for mixtures $u'/S_{L0} < 1$, the Darrieus-Landau-type bulge-cusp structures contribute to an increase in S_T/S_{L0}, and similar arguments are made by Creta et al. [29].

Bagdanavicius' experiments show that the addition of H_2, even in small amounts to CH_4 /air mixtures significantly increases S_T. A similar effect was noticed for the increase in temperature, albeit to a lesser degree (for quantitative figures and longer discussion, see Figs. 14 & 15 in their original paper). Fig. 14 also shows for higher % of hydrogen at the higher temperature of 673 K there is a shift in peak on the leaner side. The AFSW model predicts these qualitative trends, with some deviation at higher turbulence. Fig. 15 shows a

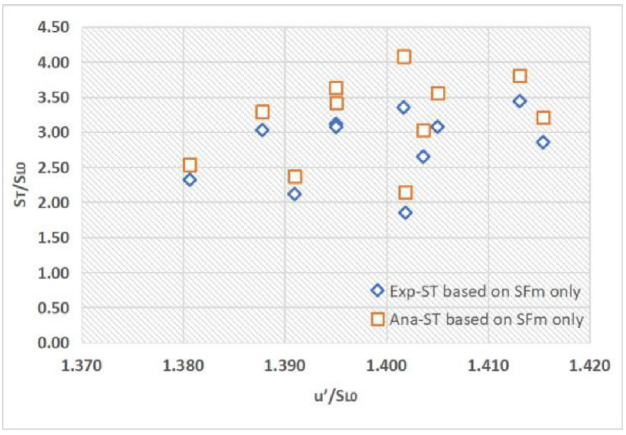

Fig. 12 (Eq. (3)) (Comparison between u'/S_{L0} vs. S_T based on SFm for 1000 rpm. i) (S_{L0} = 25.4, Le = 1, Re = 64.6); ii) (S_{L0} = 25.3, Le = 0.65, Re = 61.6); iii) (S_{L0} = 25.2, Le = 1.35, Re = 65.9); iv) (S_{L0} = 25.2, Le = 0.51, Re = 58.9); v) (S_{L0} = 25.2, Le = 0.51, Re = 58.9); vi) (S_{L0} = 25, Le = 1.59, Re = 66.4); vii) (S_{L0} = 25.1, Le = 0.4, Re = 57.4); viii) (S_{L0} = 25, Le = 0.89, Re = 63); ix) (S_{L0} = 25, Le = 0.66, Re = 60.6); x) (S_{L0} = 24.9, Le = 0.41, Re = 57.1); xi) (S_{L0} = 24.8, Le = 0.8, Re = 62.2).

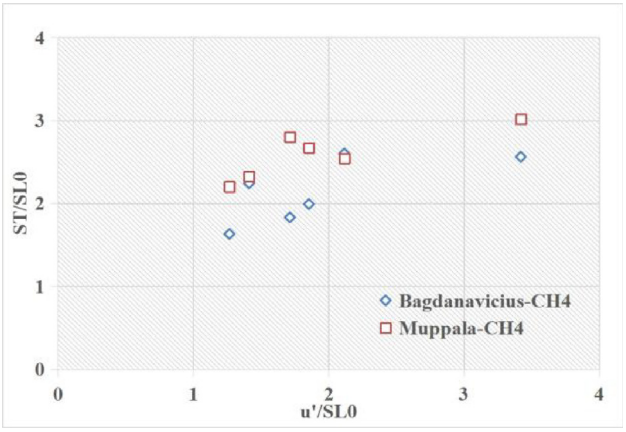

Fig. 13 Comparison between Experiment and AFSW model of Bagdanavicius data for pure CH_4 at 3 and 5 bar. (read L to R for conditions of each data): i) (573 K, 3 bar, ϕ = 0.84); ii) (473 K, 3 bar, ϕ = 0.96); iii) (673 K, 3 bar, ϕ = 0.73); iv) (573 K, 7 bar, ϕ = 0.78); v) (473 K, 3 bar, ϕ = 0.75); vi) (473 K, 7 bar, ϕ = 0.78).

slightly different behaviour. In the vicinity of $u'/S_{L0} \sim 1.5$, experiments show that S_T/S_{L0} is passive for Le numbers 0.59 to 0.72. However, the module predicts higher values for lower Le. This inconsistency gives scope for further investigation.

6. Conclusions

The algebraic flame surface wrinkling AFSW flame model predicts the closest agreements for the turbulent flame speed with both spherical expanding lean flames and geometrical Bunsen-burner flames. We conclude that the ratio of turbulence flame

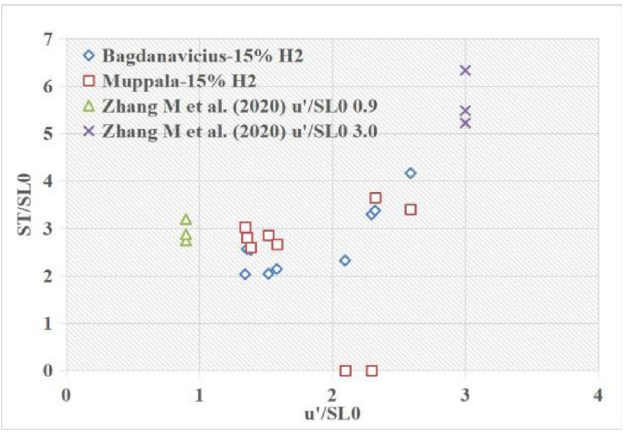

Fig. 14 Bagdanavicius data: Comparison between experiment and the AFSW model for 85% CH_4 – 15% H_2. i) (673 K, 3 bar, ϕ = 0.82); ii) (573 K, 3 bar, ϕ = 0.98); iii) (473 K, 3 bar, ϕ = 1) iv) (573 K, 3 bar, ϕ = 0.81); v) (473 K, 3 bar, ϕ = 0.82); vi) (673 K, 7 bar, ϕ = 0.79); vii) (573 K, 7 bar, ϕ = 0.99); vii) (573 K, 7 bar, ϕ = 0.8); viii) (473 K, 7 bar, ϕ = 0.86).

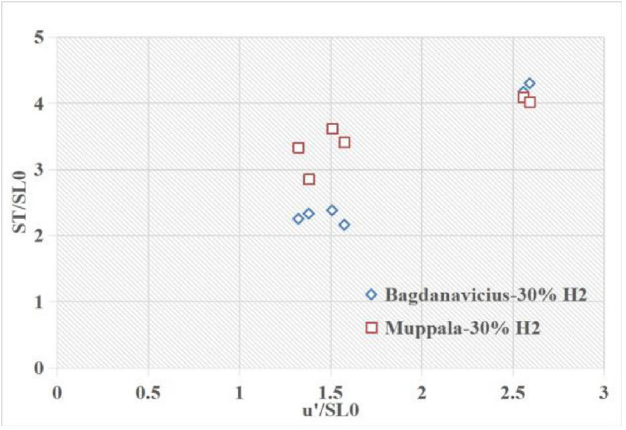

Fig. 15 Comparison between model and Bagdanavicius data, for 70% CH_4–30% H_2. i) (673 K, 3 bar, ϕ = 0.82); ii) (473 K, 3 bar, ϕ = 0.9); iii) (673 K, 3 bar, ϕ = 0.99); iv) (573 K, 3 bar, ϕ = 0.83); v) (473 K, 7 bar, ϕ = 0.99); vi) (473 K, 7 bar, ϕ = 0.85).

speed to unstretched laminar burning velocity (S_T/S_{L0}) increases proportionately with hydrogen concentration, and increases non-linearly for leaner mixtures, i.e. lower Lewis numbers. For all the data shown, the model $S_T/S_{L0} \propto \frac{1}{e^{(Le-1)}}$ predicts better than $S_T/S_{L0} \propto \frac{1}{L_e}$ for all expanding flames. The model predicts a four-fold increase in u'/S_{L0} doubles S_T/S_{L0} for both turbulence levels. The model replacing the unstretched laminar flame speed S_{L0}, with mean local burning velocity, elucidates that the influence of curved flamelets gives excellent quantification for S_T/S_{L0}.

Declaration of Competing Interest

The authors declare that they have no known competing financial interests or personal relationships that could have appeared to influence the work reported in this paper.

Acknowledgements

We are thankful to Prof. Masaya Nakahara, Ehime University, Japan, Dr Audrius Bagdanavicius, University of Leicester, UK and Dr Zhang, Xi'an Jiaotong University, China for sharing experimental data and useful discussions.

References

[1] J. Pan, G. Shu, P. Zhao, H. Wei, Z. Chen, Interactions of flame propagation, auto-ignition and pressure wave during knocking combustion, Comb Flame. 164 (2016) 319–328.
[2] H. Guo, B. Tayebi, C. Galizzi, D. Escudie, Burning Rates and Surface Characteristics of Hydrogen-Enriched Turbulent Lean Premixed Methane-Air Flames, San Francisco, California, Heat transfer summer conference, 2010, pp. 97–103.
[3] Y. Xie, Q. Li, Effect of the initial pressures on evolution of intrinsically unstable hydrogen/air premixed flame fronts, Int. J. Hydrogen Energy. 44 (31) (2019) 17030–17040.
[4] A.N. Lipatnikov, J. Chomiak, Lewis Number Effects in Premixed Turbulent Combustion and Highly Perturbed Laminar Flames, Comb Sci. Tech. 137 (1-6) (1998) 277–298.
[5] H. Kido, Study on Combustion Improvement Mechanism of Non-Stoichiometric Mixtures by Turbulence, Trans. JSME. 61 (1995) 66–71.
[6] V.P. Karpov, E.S. Severin, Effects of Molecular-transport Coefficients on the rate of Turbulent Combustion, Combustion, Explosion Shock Waves 16 (1978) 45–51.
[7] H. Kido, M. Nakahara, K. Nakashima, J. Hashimoto, Influence of local flame displacement velocity on turbulent burning velocity, Proc. Combust Inst. 29 (2) (2002) 1855–1861.
[8] M. Nakahara, H. Kido, T. Shirasuna, K. Hirata, Effect of Stretch on Local Burning Velocity of Premixed Turbulent Flames, J. Thermal Sci. Technol. 2 (2) (2007) 268–280.
[9] M. Nakahara, H. Kido, H. Jun, I. Atsushi. An experimental study on properties of local burning velocity for hydrogen added hydrocarbon premixed turbulent flames, in: ASME/JSME 2011 8th Thermal Engineering Joint Conference. 2011;article no. AJTEC2011-44039, T20105:8.
[10] H. Kido, M. Nakahara, A Model of Turbulent Burning Velocity Taking the Preferential Diffusion Effect into Consideration, JSME Int. J. Ser. B. 41 (3) (1998) 666–673.
[11] S.S. Shy, S.I. Yang, W.J. Lin, R.C. Su, Turbulent Burning Velocities of Premixed CH4/Diluent/Air Flames in Intense Isotropic Turbulence with Consideration of Radiation Losses, Comb Flame. 143 (2005) 106–118.
[12] A. Bagdanavicius, P.J. Bowen, N. Syred, P. Kay, A. Crayford, G. Sims, J. Wood, Burning velocities of alternative gaseous fuels at elevated temperature and pressure, AIAA. 48 (2) (2010) 317–329.
[13] S.P.R. Muppala, N.K. Aluri, F. Dinkelacker, A. Leipertz, Development of an algebraic reaction rate closure for the numerical calculation of turbulent premixed methane, ethylene and propane/air flames for pressures up to 1.0 MPa, Comb Flame. 140 (4) (2005) 257–266.
[14] S.P.R. Muppala, M. Nakahara, N.K. Aluri, H. Kido, J.X. Wen, M.V. Papalexandris, Experimental and analytical investigation of the turbulent burning velocity of two-component fuel mixtures of hydrogen, methane and propane, Int. J. Hydrogen Energy 34 (22) (2009) 9258–9265.
[15] F. Dinkelacker, B. Manickam, S.P.R. Muppala, Modelling and simulation of lean premixed turbulent methane/hydrogen/air flames with an effective Lewis number approach, Combustion Flame 158 (9) (2011) 1742–1749.
[16] S.P.R. Muppala, V.C. Madhav Rao, A. Mebel, V. Azyazov, Numerical Implementation and validation of turbulent premixed combustion model for lean mixtures, MATEC Web Conf. 209 (2018) 00004, https://doi.org/10.1051/matecconf/201820900004.
[17] N.K. Aluri, Numerical modelling of turbulent premixed combustion for gas turbine conditions with incorporation of molecular transport effects, University of Siegen, 2007.
[18] A. Trouvé, T. Poinsot, The Evolution Equation for the Flame Surface-Density in Turbulent Premixed Combustion, J. Fluid Mech. 278 (1994) 1–31.
[19] Y.B. Zeldovich, G.I. Barenblatt, V.B. Librovich, G.M. Makhviladze (Eds.), The Mathematical Theory of Combustion and Explosions, Springer US, Boston, MA, 1985.
[20] T. Ma, Flame Surface Density modelling for the Large Eddy Simulation of Turbulent Premixed Flames. 2013.
[21] V.L. Zimont, A.N. Lipatnikov, A Numerical Model of Premixed Turbulent Combustion of Gases, Chem. Phys. Rep. 14 (1995) 993–1025.
[22] A.N. Lipatnikov, V.A. Sabelnikov, A.Y. Poludnenko, Assessment of a transport equation for mean reaction rate using DNS data obtained from highly unsteady premixed turbulent flames, Int. J. Heat Mass Transfer 134 (2019) 398–404.
[23] R. Keppeler, E. Tangermann, U. Allaudin, M. Pfitzner, LES of Low to High Turbulent Combustion in an Elevated Pressure Environment, Flow, Turbulence Combust. 92 (3) (2014) 767–802.
[24] E. Burke, F. Güthe, R.F.D. Monaghan, A Comparison of Turbulent Flame Speed Correlations for Hydrocarbon Fuels at Elevated Pressures, in: ASME Turbo Expo. Seoul, South Korea, 2016.
[25] A.N. Lipatnikov, J. Chomiak, Molecular transport effects on turbulent flame propagation and structure, Prog. Energy Combust. Sci. 31 (1) (2005) 1–73.
[26] R.C. Aldredge, Methane-air Markstein numbers from measurements of thermoacoustic instability, Combust. Sci. Technol. 177 (5-6) (2005) 1023–1047.
[27] C. Lhuillier, P. Brequigny, F. Contino, C. Mounaïm-Rousselle, Experimental investigation on ammonia combustion behavior in a spark-ignition engine by means of laminar and turbulent expanding flames, Proc. Combust. Inst. 38 (4) (2021) 5859–5868.
[28] A.S. Betev, V.P. Karpov, A. Lipatnikov, Z.P. Vardosanidze, Hydrogen combustion in engines and preferential diffusion effects in laminar and turbulent flames, Arc Combust. 15 (1995) 188–215.
[29] F. Creta, R. Lamioni, P.E. Lapenna, G. Troiani, Interplay of Darrieus-Landau instability and weak turbulence in premixed flame propagation, Phys. Rev. E. 94 (5) (2016), https://doi.org/10.1103/PhysRevE.94.053102.
[30] G. Ozel-Erol, M. Klein, N. Chakraborty, Lewis Number Effects on Flame Speed Statistics in Spherical Turbulent Premixed Flames, Flow Turbulence Combust. 106 (4) (2021) 1043–1063.
[31] M. Brower, E. Petersen, W. Metcalfe, H.J. Curran, M. Füri, G. Bourque, N.K. Aluri, F. Güthe, Ignition delay time and laminar flame speed calculations for natural gas/hydrogen blends at elevated pressures, Proc. ASME Turbo Expo. 135 (2012) 1005–1016.
[32] M. Zhang, M. Chang, J. Wang, Z. Huang, Flame dynamics analysis of highly hydrogen enrichment premixed turbulent combustion, Int. J. Hydrogen Energy 45 (1) (2020) 1072–1083.